approximation with two-body correlations has so far been tested only for the propagation of wave functions in model system-bath Hamiltonians.[9] These models used realistic potentials with barriers very similar to those encountered in H-exchange reactions, and the test calculations showed the mean field approximation with explicit system-bath correlation to be extremely accurate over times long enough for the wave packet to move away from the saddle point region. Nevertheless, numerical calculations of rate constants for problems with three or more degrees of freedom must be carried out to verify the applicability of the approach presented here to more challenging problems. Some such applications are in progress.

Acknowledgment. This work has been supported by a Junior Fellowship from the Society of Fellows, Harvard University. The calculations reported were performed on a SUN 4/65 SPARC 1 station, funded by the Milton Fund Award of the Harvard Medical School.

Ab Initio Quantum Chemistry Study of Formamide-Formamidic Acid Tautomerization

Xiao-Chuan Wang, Jeff Nichols,† Martin Feyereisen, Maciej Gutowski, Jerry Boatz, A. D. J. Haymet, and Jack Simons*

Chemistry Department, University of Utah, Salt Lake City, Utah 84112 *(Received: April 4, 1991)*

Ab initio electronic structure calculations using analytical energy derivative methods and automated potential energy surface walking techniques have been carried out on the tautomerization reaction path connecting formamide (F) H_2N-CHO, through a transition state (TS), to formamidic acid (FA) HN-CHOH. The zero-point corrected F → FA, and F → TS energy differences are predicted to be 12.1 and 48.9 kcal/mol, respectively, when configuration interaction methods are used to treat electron correlation. An imaginary frequency of 2391*i* cm^{-1} is obtained along the reaction coordinate at the TS. Isotopic substitution of F to generate H_2N-CDO and subsequent calculation of the harmonic vibrational frequencies and eigenvectors allowed ambiguities in the assignment of the infrared spectrum of F to be resolved. The geometry of the F tautomer is found to be slightly nonplanar, but to have zero-point energy that permits the planar geometry to be dynamically accessed. Extensions to situations in which tautomerization is assisted by neighboring solvent molecule(s) are considered. In particular, the intimate involvement of a single H_2O solvent molecule reduces the zero-point-corrected F → FA and F → TS energy differences to 10.6 and 22.6 kcal/mol, respectively. Intimate solvent participation is thus found to much more strongly affect the activation energy than the overall thermodynamics in this case. The imaginary frequency corresponding to the reaction coordinate at the transition state changes to 2001*i* cm^{-1} when a single H_2O is intimately involved.

I. Introduction

Tautomerization may be facilitated in aqueous solution or in other environments containing nearby H_2O species by the transfer of a hydrogen atom (H) from one site of the solute molecule to a neighboring H_2O molecule followed by transfer of another H atom from the solvent to the second site on the solute. The transfer may be concerted or may occur in a stepwise manner and may or may not involve zwitterion like charge densities. An example of such a solvent-mediated tautomerization mechanism is illustrated in Figures 1 and 2 for the prototypical formamide-formamidic Acid (F → FA) case examined in the present work.

Of course, in solution, more than one H_2O molecule may be involved in assisting the "passage" of the H atom from one tautomeric form to the other. On the other hand, such intimate solvent-mediated mechanisms may not lower the activation energy barriers (through which H-atom tunneling may occur) enough to significantly affect the net tautomerization rate. Simple, nonintimate solvation may instead be the dominant factor controlling the activation energy and entropy as well as the tunneling rate through the activation barrier.

One of the goals of the work described here is to address such matters. In the present paper, the tautomerization of "bare" formamide and of formamide in the presence of a single H_2O solvent molecule is considered. Extensions to the case in which several H_2O molecules are involved will be treated in a forthcoming publication.

The F → FA system and similar species have been studied previously[1,2] as models for tautomerization in larger nucleic acid bases, in particular in connection with the guanine and uracil systems. Moreover, many theoretical studies employing a variety of methods have focused attention on the relative stabilities of tautomers and have examined the computed stabilities as functions of choice of basis set[3] and treatment of electron correlation.[2] Several other workers[4-6] have examined the predicted geometry of the F tautomer as a function of atomic basis set; in particular, the planarity or lack thereof at the H_2N center has been of considerable interest.

In this paper we describe the application to the F → FA tautomerization reaction of ab initio electronic structure theory and potential energy surface walking algorithms that we[7] have developed. These techniques utilize analytical energy derivatives to follow "streambeds" from a local minimum (i.e., a stable geometry) uphill to a transition state and onward to another local minimum. Since it is still experimentally unresolved[8] whether formamide is planar, the potential energy surfaces were examined both in C_1 and C_s symmetries (in C_s symmetry, an imaginary

† USI/IBM Partnership and Utah Supercomputer Institute, University of Utah, Salt Lake City, UT 84112.

(1) Kwiatkowski, J. S.; Zielinski, T. J.; Rein, R. Quantum-Mechanical Prediction of Tautomeric Equilibria *Adv. Chem. Phys.* **1986**, *18*. Minkin, V. I.; Olekhnovich, L. P.; Zhdanov, Y. A. *Molecular Design of Tautomeric Compounds*; D. Reidel Publishing Co.: Dordrecht, Holland 1988.

(2) (a) See, for example: Kwiatkowski, J. S.; Bartlett, R. J.; Person, W. B. *J. Am. Chem. Soc.* **1988**, *110*, 2353. (b) Nguyen, K. A.; Gordon, M. S.; Truhlar, D. G. University of Minnesota Supercomputer Institute Research Report UMSI 90/224. In this paper, the solvent-assisted tautomerization of formamidine (H_2N-CH-NH → HN-CH-NH_2) was examined. (c) Garrett, B. C.; Melius, C. F. NATO Advanced Study Institute on Theoretical and Computational Models for Organic Chemistry. To be published. (d) Nagaoka, M.; Okuno, Y.; Yambe, T. *J. Am. Chem. Soc.* **1991**, *113*, 769.

(3) Schegel, H. B.; Gund, P.; Fluder, E. M. *J. Am. Chem. Soc.* **1982**, *104*, 5347.

(4) Carlsen, N. R.; Radom, L.; Riggs, N. V.; Rodwell, W. R. *J. Am. Chem. Soc.* **1979**, *101*, 2233.

(5) Boggs, J. E.; Niu, Z. *J. Comput. Chem.* **1985**, *6*, 46.

(6) Radom, L.; Riggs, N. V. *Aust. J. Chem.* **1980**, *33*, 249.

(7) Nichols, J.; Taylor, H.; Schmidt, P.; Simons, J. *J. Chem. Phys.* **1990**, *92*, 340.

(8) Hirota, E.; Sugisaki, R.; Nielsen, C. J.; Sorensen, G. O. *J. Mol. Spectrosc.* **1974**, *49*, 251. Sugawara, Y.; Hamada, Y.; Tsuboi, M. *Bull. Chem. Soc. Jpn.* **1983**, *56*, 1045.

0022-3654/91/2095-10419$02.50/0

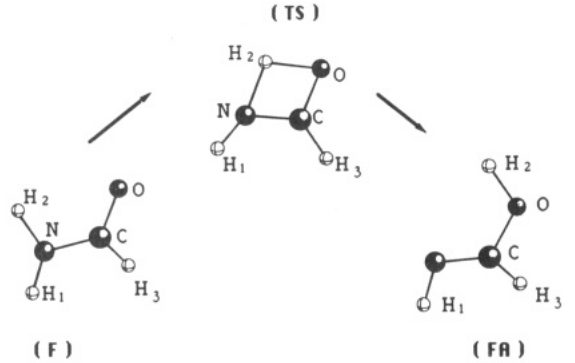

Figure 1. Tautomerization for formamide (F)–formamidic acid (FA) also showing the transition state (TS) and labeling the atoms.

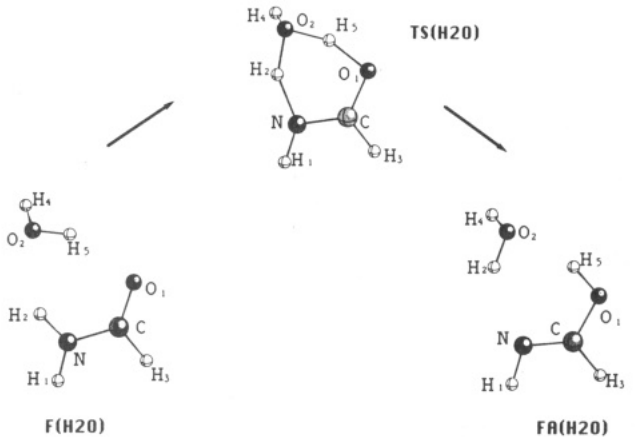

Figure 2. Tautomerization mediated by intervening H_2O molecule showing the solvated formamide F(H_2O), solvated formamidic acid FA-(H_2O), and solvent-involved transition state TS(H_2O).

vibrational frequency corresponding to out-of-plane motion provides a signature that the species has a nonplanar equilibrium geometry).

In addition, we examined the effect of H_2O molecules on the energetics (i.e., the activation barrier heights and widths (for tunneling considerations) as well as the stabilities of the two tautomers) and entropies (as embodied in the local harmonic vibrational frequencies and geometries of the tautomers and the transition state) of such reactions. In subsequent works, we expect to report analogous results for the F → FA reaction in which more than one H_2O molecule is allowed to mediate the H-atom transfer; here attention is focused on the "bare" F → FA case and on the situation with a single H_2O molecule. By first considering the reaction in the absence of solvent, we obtain a reference point from which to view solvent effects. The one-H_2O case allows us to explore whether intimate involvement of the solvent is likely to have large effects on the tautomerization activation energy and entropy as well as the H-atom tunneling rates.

II. Methods

A. Atomic Orbital Basis Sets. Earlier work has shown[1,3] that the relative stabilities of the two tautomers cannot be reliably predicted using minimal atomic orbital basis sets. We therefore employed Dunning's "correlation consistent" polarized valence double-zeta bases[9] for all of the atoms in F and FA. This basis included three s, two sets of p, and one set of d functions for each of the N, C, and O atoms, and two s and one set of p functions for each H atom. For the F and FA tautomers, a total of 60 contracted Gaussian basis functions results from this choice. The H_2O molecule added 25 contracted functions. All of the atomic-orbital integrals and integral derivatives involving this basis, as well as all other aspects of the electronic energy and analytical energy derivative evaluation, were carried out using our[10] Utah

(9) Dunning, T. *J. Chem. Phys.* **1989**, *90*, 1007.

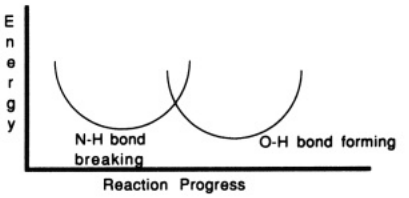

Figure 3. Schematic view of intersecting N–H and H–O diabatic energy surfaces for H_2N—CH=O → HN=CH—OH tautomerization.

MESS Kit electronic structure codes. For selected points on the potential energy hypersurface, the GAMESS[11] and MOLECULE-SWEDEN[11] codes were used to obtain additional information, including estimates of the electron correlation energies.

B. Electronic Wave Function. The tautomerization reaction involves the following qualitative changes in electronic structure: (a) A primary four-electron, three-active-orbital rearrangement within the σ framework (the initial NH bonding σ orbital, its σ^* counterpart, and the O-atom nonbonding lone-pair orbital n need to be considered, along with their four electrons; as the reaction proceeds, these orbitals evolve into the OH bonding σ and antibonding σ^* orbitals and the N-atom nonbonding n lone-pair orbital). (b) A secondary, yet important, adjustment of the four-electron N–C–O π-orbital network (in which the delocalized three-center π bonding, nonbonding, and antibonding counterparts alter their character as the tautomerization occurs).

This picture of the electronic structure changes that accompany the tautomerization process can be cast in a language to better make contact with models used in atom- and electron-transfer kinetics. In the conventional picture, one considers the movement of the H-atom center from one atom (N in the F → FA case) to another (O in this case). As the original (N–H) bond is broken, the electronic energy rises in a manner depicted qualitatively below in Figure 3. As the new (H–O) bond is formed, the electronic energy is then lowered as shown in Figure 3. Depending on the distance between the N and O atoms, the N–H and H–O diabatic potential energy curves intersect at different locations along the reaction path and at different energies.

By including the three (σ, σ^*, and n) orbitals described above, we permit the electron distribution to (1) begin with reactants N–H plus C=O in which two electrons occupy an N–H bonding orbital (σ^2) and two electrons occupy an O-atom nonbonding orbital (n^2); (2) evolve in a manner that allows the N–H bond to (at least partially) break by using the $\sigma^1\sigma^{*1}$ configuration for homolytic cleavage or the σ^2 configuration for heterolytic cleavage; (3) further evolve to begin formation of the new H–O bond, again either heterolytically or homolytically; and (4) complete the reaction by allowing two electrons to occupy the N-atom nonbonding orbital (which is now the n orbital) while placing two electrons into the H–O bonding orbital (σ^2).

This treatment of the four active electrons using three corresponding orbitals is how the present quantum chemical study permits the two "diabatic" curves depicted in Figure 3 to interact and thus produce a ground-state surface that adiabatically evolves from reactants to products. That is, our approach does not explicitly construct the diabatic potentials; it produces the adiabatic potential energy surface directly.

The H_2O-mediated case can be thought of in terms of four interacting diabatic potentials analogous to those shown in Figure

(10) The Utah molecular electronic structure system (MESS KIT) software was written during 1986–1990 by: Kendall, R. A.; Earl, E.; Hernandez, R.; Taylor, H. L.; O'Neal, D.; Nichols, J.; Hoffmann, M.; Gutowski, M.; Wang, X.; Boatz, J.; Anchell, J.; Bak, K.; Feyereisen, M.

(11) GAMESS: Dupuis, M.; Spangler, D.; Wendolowski, J. J. National Resource for Computations in Chemistry Software Catalog; Univ. of California, Berkeley, CA 1980, Program QC 01. Schmidt, M. W.; Baldridge, K. K.; Boatz, J. A.; Jensen, J. H.; Koseki, S.; Gordon, M. S.; Nguyen, K. A.; Windus, T. L.; Elbert, S. T. *Quantum Chem. Program Exchange Bull.* **1990**, *10*, 52. MOLECULE-SWEDEN:MOLECULE is a vectorized Gaussian integral program written by Almlöf, J.; SWEDEN is a vectorized SCF-MCSCF, direct CI, conventional CI-CPF-MCPF program written by: Siegbahn, P. E. M.; Bauschlicher, Jr., C. W.; Roos, B.; Taylor, P. R.; Heiberg, A.; Almlöf, J.; Langhoff, S. R.; Chong, D. P.

3. In this case, one curve represents the N–H bond that first breaks (in the presence of the intimate H_2O molecule and the neighboring C=O group), another represents the newly formed H–O bond of the H_3O or H_3O^+ moiety, the third denotes the O–H bond of the H_3O or H_3O^+ that then breaks, and the last represents the finally formed H–O bond of the H–O–CH group.

Treatment of the two additional H–O bonds that form and break in this solvent-assisted case adds to the list of active orbitals and electrons: (a) a pair of H_2O σ and σ^* orbitals as well as an H_2O nonbonding n lone-pair orbital, and (b) two pairs of electrons, two of which form a H_2O σ bond pair, the other being an H_2O lone pair. These additional orbitals and electrons thus represent a second four-electron, three-active-orbital moiety.

Both of the three-orbital four-electron rearrangements can be handled in a qualitatively correct manner at the single-configuration level; no avoided crossings of configurations arise to necessitate a two or more configuration treatment. Likewise, the polarization of the four-electron three-orbital π-framework can be treated within a single-configuration description. This does not mean that electron correlation effects are unimportant; it simply means that these species do not require a multiconfiguration reference wave function to achieve a qualitatively correct picture of the reaction.

For these reasons, we have carried out single-configuration ab initio electronic structure calculations on the F → FA reaction path, with and without the H_2O molecule. Upon locating the stationary points (i.e., the F and FA minima and the transition state TS) and calculating local harmonic vibrational frequencies on this single-configuration "reference function" surface, we employed both the configuration interaction with single and double excitations from the single configuration reference function (CISD) method and the second-order Møller–Plesset perturbation theory (MP2) method to evaluate the electron correlation energies of these species.

Earlier workers[1,2b,12-15] have examined the role of solvation in determining the relative stabilities of tautomers, using a variety of ab initio and semiempirical approaches. In the present work, we have chosen to employ the so-called "supermolecule" approach in which the solute and solvent are treated as one entity. By comparing the relative energetics predicted for the F, FA, and TS structures (or their solvated analogues) at the CISD and MP2 levels of theory, we gain an evaluation of whether large "size extensivity" errors are present in our approach.

C. Potential Surface Walking Strategy. The potential energy surface walking algorithm outlined in ref 7 uses local analytical first and second energy derivatives (i.e., gradients and Hessians) to develop a series of "steps" that can lead (1) from a starting geometry "downhill" in energy along all internal degrees of freedom to a local minimum, or (2) from a local minimum, "uphill" along one eigenmode of the local Hessian while moving downhill along all other eigenmodes, to a transition state. By following such streambeds on the reaction potential energy surface, this process allows us to trace out paths that connect the two tautomers via their transition state. Calculation of the local Hessian also permits us to evaluate local harmonic vibrational frequencies for the two tautomers and the transition state.

In the present study of the H_2O-assisted tautomerization, we searched for streambeds that might describe reaction paths of the following types:

1. A path which is dominated by N–H bond stretching early in the reaction with relatively little distortion of the H_2O solvent, followed by O–H bond cleavage within the H_2O moiety. Such a path can be viewed as describing a stepwise N–H (HOH) O=C → N (H_2OH) O=C → N (H_2O) H-OC process (but not one in which stable intermediates are found).

2. A path which is dominated by solvent molecule O–H bond stretching and corresponding H–OC bond formation early in the reaction, followed by N–H bond cleavage to restore the HOH solvent species. Such a path can be viewed as describing a stepwise N–H(HOH)O=C → N–H(HO)H–OC → N(H_2O)H–OC process (but not one in which stable intermediates are found).

3. A fully concerted path in which the N–H bond is broken in concert with (i) formation of a new H–O bond in the solvent, (ii) breaking of another O–H bond in the solvent, and (iii) formation of the H–OC bond.

Our early efforts to locate the solvent-assisted transition state were aided by carrying our "point-by-point" energy calculations at a grid of geometries in which only the two hydrogen atoms numbered H_2 and H_5 were displaced along directions designed to move them from an initial N–H_2 and O–H_5 arrangement to a final H_2–O and H_5–O arrangement (see Figure 2). From this grid of energies and geometries we were able to identify candidate geometries at which successful transition-state searches using the above algorithm could be achieved.

TABLE I: SCF Calculated and Experimental Interatomic Distances (Å) for the Tautomers and the Transition State

bond	formamide calcd	formamide expt	transition state (calcd)	formamidic acid (calcd)
C–O	1.1885	1.193,[a] 1.219[b]	1.2592	1.3296
C–N	1.3537	1.376, 1.352	1.2882	1.2477
C–H_3	1.1011	1.102, 1.098	1.0871	1.0885
N–H_1	0.9970	1.002, 1.002	1.0002	1.0072
N–H_2	1.0000	1.014, 1.002	1.3091	2.2956
O–H_2	2.5105		1.3037	0.9511

[a] Costain, C. C.; Dowling, J. M. *J. Chem. Phys.* **1960**, *32*, 158. [b] Hirota et al. (ref 8).

TABLE II: SCF Calculated and Experimental Interatomic Angles (deg) for the Tautomers and the Transition State

interatomic angle	formamide calcd	formamide expt	transition state (calcd)	formamidic acid (calcd)
∠CNH_1	120.20	120.0	125.86	110.87
∠CNH_2	117.95	117.1,[a] 118.5[b]	73.25	53.80
∠OCN	124.99	123.8, 124.7	108.12	122.55
∠OCH_3	122.46	123.0, 122.5	123.50	110.66
∠NH_3	112.54	113.2, 112.7	128.38	126.78
∠H_1NH_2	117.99	118.9, 121.6	160.89	164.67
∠H_2OC	52.73		74.38	107.75

[a] Costain, C. C.; Dowling, J. M. *J. Chem. Phys.* **1960**, *32*, 158. [b] Hirota et al. (ref 8).

III. Results

A. Energetic Stabilities and Structures. 1. F, FA, and TS. The SCF-optimized bond lengths and angles of the formamide (F), formamidic acid (FA), and transition state (TS) are described respectively in Tables I and II. For the F molecule, experimental structural data are included for comparison; analogous data are, to our knowledge, not available for the FA tautomer, and are, of course, absent for the TS. Notice that, as the tautomerization proceeds, all of the bond lengths except the CH and NH_1 lengths change significantly; this, of course, is consistent with the substantial changes in electronic structure expected based on the discussion of section II.B.

Our SCF-level data (see Table III) indicate that the nonsolvated F → FA tautomerization reaction has an *electronic* endothermicity of 12.2 kcal/mol and an activation energy of 60.3 kcal/mol. When corrected for zero-point energies using the SCF harmonic vibrational frequencies given in Tables IV–VII, these SCF-level energy differences change to 12.9 and 57.3 kcal/mol, respectively.

Our CISD correlated estimates (see Table III) of these same energy differences (zero-point corrected using the SCF vibrational frequencies) are 12.1 and 48.9 kcal/mol, respectively. The de-

(12) Clementi, E.; Cavallone, F.; Scordamaglia, R. *J. Am. Chem. Soc.* **1977**, *99*, 5531.
(13) Duben, A. J.; Miertus, S.; *Chem. Phys. Lett.* **1982**, *88*, 395. Duben, A. J.; Miertus, S. *Theor. Chim. Acta (Berlin)* **1981**, *60*, 327.
(14) Del Bene, J. E. *J. Chem. Phys.* **1975**, *62*, 1961. Hinton, J. F.; Harpool, R. D. *J. Am. Chem. Soc.* **1977**, *99*, 349. Peinel, G. *Stud. Biophys.* **1983**, *93*, 205. Hofmann, H. J.; Peinel, G.; Weller, G. *Int. J. Quantum Chem.* **1979**, *16*, 379.
(15) Löwdin, P. O. *Rev. Mod. Phys.* **1963**, *35*, 724.

TABLE III: Total Energies (atomic units) at Stationary Points for SCF and Correlated Wave Functions and Energy Differences for Solvated and Unsolvated Species (kcal/mol)

A. Total Energies

species	SCF	CISD-(FULL)[a]	CISD-(FCOR)[b]	MP2[c]
F	−168.949 65	−169.410 35	−169.400 53	−169.4467
FA	−168.930 20	−169.392 18	−169.382 53	−169.4279
TS	−168.853 53	−169.327 72	−169.318 18	−169.3746
$F(H_2O)$	−244.992 40	−245.624 80	−245.612 07	−245.7008
$FA(H_2O)$	−244.975 08	−245.609 50	−245.596 90	−245.6861
$TS(H_2O)$	−244.936 03	−245.583 37	−245.570 78	−245.6707

B. Energy Differences

species	SCF	CISD-(FULL)	CISD-(FCOR)	MP2	ΔZPE[d]
F → FA	12.2	11.4	11.3	11.8	0.7
F → TS	60.3	51.9	51.7	45.2	−3.0
$F(H_2O)$ → $FA(H_2O)$	10.9	9.60	9.52	9.22	1.0
$F(H_2O)$ → $TS(H_2O)$	35.4	26.0	25.8	18.9	−3.4

[a] With all electrons treated at the singles-and-doubles configuration interaction level. [b] With three frozen core orbitals (carbon, nitrogen, and oxygen 1s) not included in the correlation treatment. [c] Using second-order Møller–Plesset perturbation theory. [d] The difference in zero-point energies between the pair of species. Thus, for example, the zero-point-corrected $F(H_2O)$ → $TS(H_2O)$ energy difference is 26.0 − 3.4 = 22.6 kcal/mol at the CISD level.

TABLE IV: Vibrational Frequencies of Formamide (cm^{-1})

calcd	assignment	expt[e]	assignment
254	NH_2 wagging	289[a]	NH_2 wagging
615	NCO bending and NH_2 twisting	581[b]	NCO bending
661	NH_2 twisting and NCO bending	603[b]	NH_2 twisting
1147	NH_2 rocking and CH out-of-plane def	1021[c]	CH out of plane def
1180	CH out-of-plane def and NH_2 rocking	1046[d]	NH_2 rocking
1367	CN stretch	1258	CN stretch
1537	CH bending	1390	CH bending
1745	NH_2 scissoring	1577	NH_2 scissoring
1992	CO stretching	1754	CO stretching
3162	CH stretch	2854	CH stretch
3801	NH_2 sym stretching	3439	NH_2 sym stretching
3945	NH_2 antisym stretch	3563	NH_2 antisym stretch

[a] King, S. T. *J. Phys. Chem.* **1971**, *75*, 405. [b] As discussed in ref 8, the NCO bending and NH_2 twisting are thought to be involved in Coriolis interaction. [c] As discussed in ref 8, this assignment is not supported by their observations. [d] This band has an anomalous shape which may be due to Coriolis coupling. [e] Sugawara et al. (ref 8).

pendence of our correlated-level results on the method used to treat electron correlation is demonstrated in Table III where our CISD and MP2 energies for the F, FA, and TS structures are shown; we view our CISD results as the most reliable.

2. $F(H_2O)$, $FA(H_2O)$, and $TS(H_2O)$. For the H_2O-assisted tautomerization reaction, we find a CISD-level $F(H_2O)$ → $FA(H_2O)$ electronic energy difference of 9.60 kcal/mol and a $F(H_2O)$ → $TS(H_2O)$ electronic activation energy of 26.0 kcal/mol. The corresponding zero-point corrected energies are 10.6 and 22.6 kcal/mol. The $F(H_2O)$, $FA(H_2O)$, and $TS(H_2O)$ SCF-optimized geometries are shown in Table VIII, and the corresponding SCF harmonic vibrational frequencies are displayed in Tables IX–XI.

B. Vibrational Frequencies and Assignments. The local harmonic vibrational frequencies of F, as well as our assignments based upon analysis of the corresponding vibrational eigenvectors, are described in Table IV. Because we have not included any treatment of anharmonicities and because the harmonic frequencies are computed at the SCF level, caution must be exercised when using our results. The SCF approximation often overestimates vibrational frequencies by 10%; especially for low-frequency vibrations such as the H_2N out of plane bending motion, anharmonicities are likely to be very important.

Experimental data for the vibrational frequencies are also presented for comparison. In Table V analogous data are given for the deuterated F species H_2NCDO. This particular deuterated species was examined because the vibrations whose assignments are in doubt[8] involve motion of the C–D bond; consideration of this isotopic variant helped us in assigning the vibrational frequencies in question. In Tables VI and VII, the local harmonic vibrational frequencies and our assignments are provided for the FA and TS structures. All of the data of Tables IV–VII pertain to the C_1 symmetry case.

TABLE V: Vibrational Frequencies of Deuterated Formamide H_2NCDO (cm^{-1})

calcd	assignment	expt[a]	assignment
254	NH_2 wagging	not obsd	
606	NCO bending and NH_2 twisting	563[b]	NCO bending
648	NH_2 twisting and NCO bending	591[b]	NH_2 twisting
990	CD out-of-plane def	955	CD bending
1049	DCO bending + NH_2 rocking	c	CD out of plane def
1238	NH_2 rocking	1142	NH_2 rocking
1358	CN stretch + DCO and CNH bending	1242	CN stretch
1740	NH_2 scissoring	1582	NH_2 scissoring
1964	CO stretching	1740	CO stretching
2355	CD stretch	2135	CD stretch
3801	NH_2 sym stretching	3438	NH_2 sym stretching
3945	NH_2 antisym stretch	3563	NH_2 antisym stretch

[a] Sugawara et al. in ref 8. We find interactions between the NCO bending and NH_2 twisting motions as well as between the CN stretching and CNH and DCO bending motions. We are confident in assigning 990 cm^{-1} as the CD out-of-plane deformation mode, but 1049 cm^{-1} we are less certain of. It seems to involve coupling between the DCO bending and the NH_2 rocking motions. [b] As discussed in ref 8, the NCO bending and NH_2 twisting are thought to be involved in Coriolis interaction. [c] The intensity of this peak was too low to resolve and assign.

TABLE VI: Vibrational Frequencies of Formamidic Acid (cm^{-1})

calcd	assignment
638	NCO bending
641	OH out of plane
908	OPA[a] (H_3,C,O_1,N) and OPA(H_3,C,N,H_1) and torsion[b](N,C,O_1H_2)
1170	CO_1 stretching and CNH_1 bending
1182	OPA(H_3,C,O_1,N) and OPA(H_3,C,N,H_1)
1304	CNH_1, O_1CH_3, and CO_1H_2 bending
1479	CO_1H_2, O_1CH_3, and CNH_1 bending
1536	CNH_1 and O_1CH_3 bending
1917	CN stretching and O_1CH_3 bending
3300	CH stretching
3758	NH stretching
4084	OH stretching

[a] Here and in other tables, the notation OPA(I,J,K,L) is used to denote motion of the angle between a bond connecting atoms I and J and the plane containing atoms J, K, and L. [b] Torsion(I,J,K,L) denotes motion of the torsion angle between the planes containing atoms I, J, and K and atoms J, K, and L.

TABLE VII: Vibrational Frequencies of the Transition State (cm^{-1})

calcd	assignment
2391*i*	N–H–O movement[a]
505	N–H out-of-plane def
954	O_1CN and CNH_1 bending
1168	OPA(H_3,C,O_1,N)
1215	CNH_1 and O_1CH_3 bending
1233	torsion(H_2,N,C,O_1)
1312	O_1CH_3 and CNH_1 bending and CO_1 stretching
1594	CO_1 and CN stretching and CNH_1 bending
1763	CO_1 and CN stretching and O_1CH_3 bending
2342	NH_2 stretching and CNH_2 bending
3338	C–H stretching
3845	N–H stretching

[a] Imaginary frequency corresponding to the reaction coordinate.

TABLE VIII: SCF Calculated Interatomic Distances (Å) and Angles (deg) for the Hydrated F, FA, and TS Species

distance	$F(H_2O)$	$FA(H_2O)$	$TS(H_2O)$
$C-O_1$	1.1997	1.3164	1.2598
C–N	1.3405	1.2558	1.2943
$C-H_3$	1.0994	1.0889	1.0936
O_1-H_5	2.5172	0.9607	1.2509
O_1-O_2	2.9098	2.8273	2.3567
$N-H_1$	0.9959	1.0063	1.0005
$N-H_2$	1.0041	2.1149	1.3304
$N-O_2$	2.9948	2.8965	2.3905
H_2-O_2	2.1543	0.9556	1.1545
O_2-H_4	0.9465	0.9471	0.9482
O_2-H_5	0.9540	1.9090	1.1563
angle	**$F(H_2O)$**	**$FA(H_2O)$**	**$TS(H_2O)$**
$\angle CNH_1$	120.65	110.80	116.05
$\angle CNH_2$	118.75	106.55	104.43
$\angle O_1CN$	125.17	123.82	122.07
$\angle NCH_3$	113.49	125.01	120.77
$\angle H_4O_2H_5$	104.72	109.64	105.39
$\angle O_2H_4N$	44.81	49.84	47.70

TABLE IX: Vibrational Frequencies of $F(H_2O)$ (cm^{-1})

calcd	assignment
125	torsion(O_2,H_4,N,H_2)
160	O_2H_2 stretching
174	O_2H_5N bending
203	$H_4O_2H_2$ bending
312	torsion(O_1,C,N,H_1)
381	torsion(H_5,O_2,H_2,N)
637	$H_5O_2H_2$ bending
654	O_1CN bending
781	torsion(H_2,N,C,H_3)
1178	CN stretch, H_2NC bending and OPA(N,C,O_1,H_3)
1185	OPA(N,C,O_1,H_3)
1410	CO_1 stretch and H_2NC bending
1534	NCH_3 bending
1751	H_2NC bending and H_1NC bending
1800	torsion(H_5,O_2,H_2,N)
1949	CO_1 stretch
3181	CH_3 stretch
3752	NH_2 stretch
3939	NH_1 stretch
4020	O_2H_5 stretch
4175	O_2H_4 stretch

TABLE X: Vibrational Frequencies of $FA(H_2O)$ (cm^{-1})

calcd	assignment
179	torsion(O_2,H_2,N,H_1)
191	O_2H_2N bending
202	H_2O_2 stretch
286	$H_4O_2H_2$ bending and torsion(O_2,H_2,N,H_1)
360	torsion(H_4,O_2,H_2,N) and torsion(H_5,O_2,H_2,N)
677	$H_5O_2H_2$ bending
691	O_1CN bending
860	torsion(H_3,C,N,H_2), torsion(O_1,C,N,H_1), and torsion(O_2,H_2,N,H_1)
907	OPA(N,C,O_1,H_3)
1191	OPA(N,C,O_1,H_3) and torsion(H_3,C,N,H_2)
1200	CO_1 stretch and H_1NC bending
1375	H_3CN bending, H_1NC bending, and CO_1 stretch, and NH_2 stretch
1542	NCH_3 bending, CN stretch and NH_2 stretch
1565	NCO_1 bending, H_1NC bending and NH_2 stretch
1789	torsion(H_4,O_2,N,H_2) and torsion(H_4,O_2,N,H_2)
1894	CN stretch, CO_1 stretch, and H_3CN bending
3295	CH_3 stretch
3765	NH_1 stretch
3879	H_2NC bending
3995	O_2H_5 stretch
4169	O_2H_4 stretch

The vibrational frequencies obtained in the (constrained planar) C_s case are all within a few percent of those reported here for the (unconstrained) C_1 case, except for the 253.9-cm^{-1} NH_2 wagging vibration, which, in C_s symmetry becomes an (unstable) imaginary-frequency vibration with $\omega = 183i$ cm^{-1}. This clearly indicates that the planar structure of the F molecule is not a local minimum on the electronic energy surface. However, the total electronic energy of the planar F tautomer differs by only 12 cm^{-1} from the nonplanar minimum-energy F structure. This energy difference is far less than the zero-point energy of the NH_2 wagging motion, so a planar geometry is probably the "dynamical" equilibrium structure.

TABLE XI: Vibrational Frequencies of $TS(H_2O)$ (cm^{-1})

calcd	assignment
2010*i*	O_1H_5, NH_2, O_2H_2, and O_2H_5 stretch
291	torsion(H_5,O_1,C,N)
523	OPA(H_4,O_2,H_5,H_2)
589	O_1H_5 and NH_2 stretch, and CO_1H_5 bending
628	H_5O_1 and H_5O_2 stretch
676	$H_4O_2H_5$ bending and torsion(C,N,H_2,O_2)
745	OPA(H_1,N,C,H_2)
761	H_2N and O_2H_2 stretch and H_5O_1C bending
1073	O_2H_2 and NH_2 stretch
1186	OPA(H_1,C,O_1,N)
1282	CNH_1 bending and CO_1, H_2O_2 and CN stretch
1441	O_1CH_3 bending and CO_1 stretch
1492	torsion(C,N,H_2,O_2), $O_1H_5O_2$, $H_4O_2H_5$, and NH_2O_2 bending
1594	NC stretch and CNH_1 bending
1630	torsion(H_2,O_2,H_5,O_1), and torsion(C,N,H_2,O_2) and OPA(H_4,O_2,H_5,H_2)
1753	CO_1 stretch, and $H_4O_2H_5$ and O_2H_2N bending
1896	CN and CO_1 stretch and O_2H_2N and $O_1H_5O_2$ bending
2129	O_2H_2N, $O_1H_5O_2$, and CO_1H_5 bending
3250	CH_3 stretch
3841	NH_1 stretch
4131	O_2H_4 stretch

For the H_2O-containing species, the stationary-point geometries are given in Table VIII, and the SCF local harmonic vibrational frequencies are shown in Tables IX–XI. In addition to the $F(H_2O)$ and $FA(H_2O)$ structures shown in these tables, several other local minima were located. These minima, which involve different location of the H_2O solvent molecule, suggest alternative sites where H_2O molecules are likely to reside when more than one solvent molecule is present. Their geometries and energies will not be detailed here; rather, a subsequent publication dealing with F, FA, and TS in the presence of many H_2O molecules will provide these details.

C. Comparison with Results of Other Workers. The SCF-level energies of F and FA obtained by the Bartlett group[2] using a 6-31G* basis are −168.929 912 and −168.905 808, which yield a F → FA electronic energy difference of 15.1 kcal/mol. Their F → FA correlation energy differences (which they obtained at several levels of correlation), all favor FA over F but by no more than 1.5 kcal/mol. Considerations of zero-point vibrational energies were found to affect the F → FA energy difference by less than 2.5 kcal/mol. Therefore, these earlier workers[1] arrived at F → FA correlated-electronic-plus-zero-point energy differences of 13.6–15.1 kcal/mol (recall that we obtain 12.1 kcal/mol). The geometries obtained by these workers (for those degrees of freedom that they optimized) for the two tautomers are quite close to those reported here in Tables I and II (although they force both the F and FA species to remain planar).

Schlegel et al.,[3] using Møller–Plesset perturbation theory to estimate correlation energies and including zero-point corrections, find F → FA to be endothermic by 12 kcal/mol. Both Radom and Riggs[6] and Boggs and Niu[5] examined the geometry of F and found it to be nonplanar, but with a very small (≤1 kcal/mol) energy required to reach the planar geometry. These findings, as well as those of the Bartlett study, are in agreement with our findings. Using the best available experimental data for analogue compounds, Schlegel estimates[3] the F → FA energy difference as 11 ± 4 kcal/mol, which again is in agreement with our best estimates.

The tautomeric energy differences and geometries of uracil were recently investigated[16] using 6-31G** bases and SCF (for geom-

(16) Gould, I. R.; Hillier, I. H. *J. Chem. Soc., Perkins Trans.* **1990**, *2*, 329.

etry optimization) as well as second-order Møller–Plesset perturbation theory treatments of the electronic structure. The 2-oxo-4-oxo form was found, when correlation and zero-point energies were included, to be 10.9 kcal/mol more stable than the 2-hydroxy-4-oxo form and 12.4 kcal/mol more stable than the 2-oxo-4-hydroxy form. In ref 16 reference is made to simulation studies[17] that obtain solvation effects on tautomeric energy differences for uracil-like compounds of approximately 4.8 kcal/mol.

To the best of our knowledge, the isolated-molecule F → TS activation energy has not been determined by other workers. If our value of 48.9 kcal/mol is accurate, it would be very difficult to measure the rate of tautomerization experimentally at any accessible temperature. A 48.9 kcal/mol barrier is simply too large to be passed, even when tunneling is taken into account, at any appreciable rate at room temperature. In contrast, the 22.6 kcal/mol barrier predicted for the solvent-assisted case should produce much higher interconversion rates. This lowering of the activation energy by more than 26 kcal/mol is very large and represents one of the more important predictions of this paper.

The difference between the F → FA and F(H_2O) → FA(H_2O) CISD energies (12.1 and 10.6 kcal/mol, respectively) is not as great as the corresponding change in activation energy discussed above. However, even these changes are large enough to significantly affect the equilibrium concentration predicted for the unfavored FA tautomer.

Recently, Nguyen et al. studied[2b] the H_2O-assisted tautomerization of formamidine (H_2N–CH–NH → HN–CH–NH_2) which is closely related to the F → FA tautomerization treated here. They find zero-point-corrected activation energies in the range of 40–44 kcal/mol for the non-solvent-assisted case. When a single H_2O molecule is involved, their activation energy (the energy difference between the H_2O···H_2N–CH–NH complex and the transition state) reduces to 17–21 kcal/mol; this reduction in activation energy of ca. 20 kcal/mol is large but not as large as the 26 kcal/mol we find for the formamide case.

Moreover, Garrett and Melius[2c] combined ab initio electronic structure calculations and variational transition-state theory to examine hydrolysis of formaldehyde involving either a single solvent molecule (H_2CO···H_2O → $H_2C(OH)_2$) or assisted by participation of a second water molecule (H_2CO···$(H_2O)_2$ → $H_2C(OH)_2$···H_2O). These authors found a large activation energy reduction of 20 kcal/mol, very much in line with what Nguyen et al. and we have found. Nagaoka et al.[2d] also examined the formamide water system using molecular dynamics techniques.

In our future work on the F → FA tautomerization, we will examine the effects of more than one solvent molecule on the F, FA, and TS structures. It will be especially important to determine the differential solvation energies of the F and TS species, because this energy determines the rate at which the favored F tautomer can rearrange to FA. Of course, the relative energies of the solvated F and FA species is also of much interest. Both the rates and the equilibrium concentration of the unfavored FA tautomer, play important roles in mechanisms thought to lead to spontaneous mutations.[15]

(17) Cieplak, P.; Bash, P.; Singh, U. C.; Kollman, P. A. *J. Am. Chem. Soc.* **1987**, *109*, 6283.

IV. Summary

Using correlation-consistent polarized valence double-zeta atomic orbital bases, a single-configuration electronic wave function, analytic energy derivatives, and our potential energy surface walking algorithm, we have determined the equilibrium structures, energies, and local harmonic vibrational frequencies of "gas-phase" formamide (F), formamidic acid((FA), and the transition state (TS) connecting these tautomers. The F → FA reaction is predicted to be endoergic by 12.1 kcal/mol and to have an activation energy of 48.9 kcal/mol. In the presence of a single intimately involved H_2O molecule, these energy differences are reduced to 10.6 and 22.6 kcal/mol, respectively. The change in the activation energy is very large and suggests that participation by neighboring H_2O molecules in the tautomerization process is likely to be very important. The minimum-energy structure of F is found to be slightly nonplanar at the H_2N center, but the out-of-plane zero-point vibrational motion can easily access the planar structure. New assignments of the experimentally observed infrared spectrum of the F tautomer were made possible by carrying out eigenvector analysis of the mass weighted Hessian for the H_2N–CDO isotopically substituted species.

In future work we intend to consider both (i) the possibility that a pair of intimately involved H_2O molecules may be even more effective in lowering the activation energy (consideration of molecular sizes based on covalent radii show that two water molecules can indeed 'fit' between the H–N group and the C=O moiety), and (ii) the possibility that FA dimers may be involved in effecting tautomerization (analogous studies described in refs 2a and 2b indicate that dimer formation can greatly facilitate proton transfer). Of course, in the latter case, the tautomerization rate will depend on the concentration of the FA monomer and the 2FA ↔ equilibrium constant.

Acknowledgment. This work was supported in part by the Office of Naval Research and by NSF Grant CHE8814765. We thank the Utah Supercomputer Institute for staff and computer resources and Dr. R. Kendall of The Battelle Northwest Labs for help in obtaining the SDCI results for the TS(H_2O) species.

Registry No. D_2, 7782-39-0; H_2O, 7732-18-5; formamide, 60100-09-6; formamidic acid, 75-12-7.